THE ARNO MODEL

By Prof. Ezio TODINI
Department of Earth and Geo-Environmental Sciences
University of Bologna, Bologna, Italy

ABSTRACT: The paper describes the ARNO model, a continuous time semi-distributed rainfall-runoff model, widely used in the last two decades as the basic tool for several applications such as water master planning, analysis of extreme floods, realisation of real-time flood forecasting systems and last but not least to represent the soil component in General Circulation Models (GCM). The ARNO model is based upon a parametric description of the main hydrological processes taking place at the catchment scale, such as infiltration, evapo-transpiration, drainage, percolation, routing, etc., and can represent a large catchment as a tree shaped cascade of sub-catchments. The paper will also briefly discuss the parameter calibration and present the application of the ARNO model to the Tiber river in Italy.

1. INTRODUCTION

Most discrete time rainfall-runoff models operable over long uninterrupted periods can be classified as Explicit Soil Moisture Accounting models, ESMA, and of these models probably the most famous is the Stanford Watershed Model (Crawford and Linsley, 1966). In a typical ESMA-type model the soil moisture storage is modelled as three reservoirs: upper zone, lower zone, and active or deep groundwater storage, and the overland flow occurs from impervious as well as from non-impervious areas. The channel flow routing in ESMA type models is either a Muskingum routing, a kinematic wave, or more frequently an arbitrary linear transfer function. The more complex ESMA models usually make provision for multiple sub-watershed inputs within the channel routing phase. Various other mechanisms are provided by most ESMA type models that tend to make the overall model highly non-linear. Unfortunately the ESMA type

models have been over-parameterised and as reported by the WMO inter-comparison of conceptual models (1975) and by Franchini and Pacciani (1991) the large number of parameters is not directly related to improved performances or to better physical representations.

In the late seventies Zhao (1977) showed how the formation of runoff, in regions not suffering from prolonged dryness, was highly related to the dynamics of saturated surfaces as a function of the precipitation volumes, and he developed the Xinanjiang model, which was widely and successfully used in China; similar results were also found by Moore and Clarke (1981) who developed the Probability Distributed Soil Capacity model. Following the work of Zhao, Todini (1988) found that a major improvement could be obtained by allowing the soil moisture to be depleted not only by evapotranspiration, as in the original Xinanjiang, but also by drainage into the river network and percolation into the water table.

This gave rise to a new conceptual model, which was developed by Todini (1988) within the frame of the hydrological study of the river Arno on behalf of the Tuscany Regional Government in Italy, from which the name of ARNO model.

2. DESCRIPTION OF THE ARNO MODEL

The ARNO model is a tentative of setting up a comprehensive framework for describing most of the processes lumped at catchment or sub-catchment scale. The processes represented in the ARNO model are the following:

- Soil moisture balance
- Drainage
- Percolation
- Groundwater
- Evapo-transpiration
- Snow accumulation and melting
- Parabolic overland runoff routing
- Parabolic in stream routing

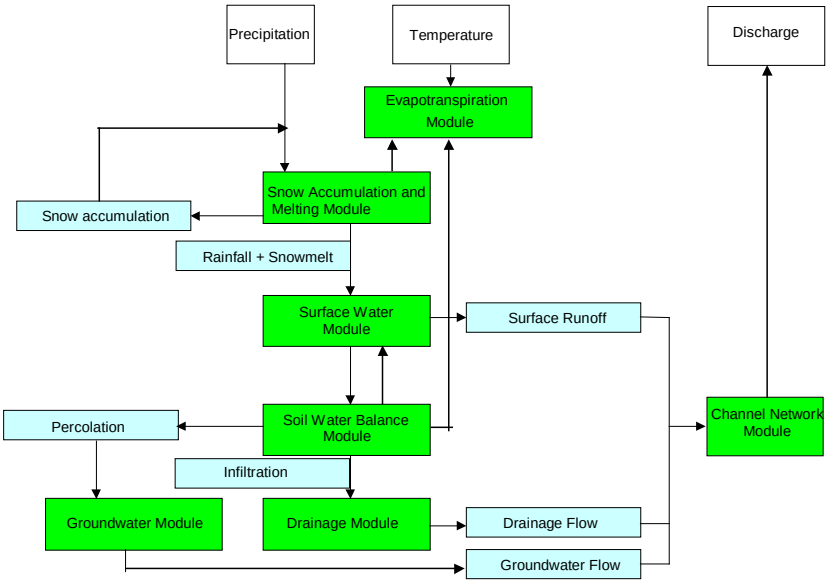

Fig. 1. A flowchart representing the ARNO model

Figure 1 shows a flow chart representing the data, the processes and the modules used in the ARNO model. These modules are described in the sequel, together with their parameterisation and the relevant assumptions made, while the full derivation of the equations reported in this paper can be found in Todini (1996).

2.1. Soil Moisture Balance Module

As pointed out by Dooge (1973) and also shown by Todini and Wallis (1977) the major problem in representing the rainfall runoff process lies in the strongly non-linear behaviour and feed-back due to the soil moisture storage, which controls the runoff production. This is why the different rainfall runoff are qualified and distinguished on the basis of the soil moisture balance representation they adopted. The soil moisture balance module of the ARNO model derives from the Xinanjiang model developed by Zhao (1977, 1984), who expressed the spatial distribution of

the soil moisture capacity in the form of a probability distribution function, similar to that advocated by Moore and Clarke (1981) and Moore (1985). Successively, in order to account more effectively for soil depletion due to drainage, this model scheme was modified by Todini (1988), who originated the ARNO model within the frame of the hydrological study of the river Arno.

The basic assumptions expressed in the soil moisture balance module of the ARNO model are:

- the precipitation input to the soil is considered uniform over the catchment (or sub-catchment) area;
- the catchment is composed of an infinite number of elementary areas (each with a different soil moisture capacity and a different soil moisture content) for each of which the continuity of mass can be written and simulated over time;
- all the precipitation falling over the soil infiltrates unless the soil is either impervious or it has already reached saturation; the proportion of elementary areas which are saturated is described by a spatial distribution function;
- the spatial distribution function describes the dynamics of contributing areas which generate surface runoff;
- the total runoff is the spatial integral of the infinitesimal contributions deriving from the different elementary areas;
- the soil moisture storage is depleted by the evapo-transpiration, by lateral sub-surface flow (drainage) towards the drainage network and by the percolation to deeper layers;
- both drainage and percolation are expressed by simple empirical expressions.

A sub-basin of given surface area S_T (excluding the surface extent of water bodies such as reservoirs or lakes) is in general formed by a mixture of pervious and less pervious soils, the response to precipitation of which will be substantially different. For this reason the total area S_T is divided into the impervious

area S_I and the pervious area S_P :

$$S_T = S_I + S_P \tag{1}$$

In order to derive the expressions needed for the continuous updating of the soil moisture balance, let us first deal with the amount of precipitation that falls over the pervious area. Given that from equation (1) the entire pervious area is:

$$S_p = S_T - S_I \tag{2}$$

if one denotes by (S - S_I) the generic surface area at saturation, x, defined as:

$$x = \frac{S - S_I}{S_T - S_I} \tag{3}$$

will indicate the proportion of pervious area at saturation. Zhao (1977) demonstrated that the following relation holds reasonably well between the area at saturation and the local proportion of maximum soil moisture content w/w_m, where w is the elementary area soil moisture at saturation and w_m is the maximum possible soil moisture in any elementary area of the catchment.

$$x = 1 - \left(1 - \frac{w}{w_m}\right)^b \tag{4}$$

This can be inverted to give the cumulative distribution for the elementary area soil moisture at saturation, shown in Figure 2 and defined as:

$$w = w_m \left[1 - (1 - x)^{\frac{1}{b}}\right] \tag{5}$$

In the ARNO model, an interception component (Rutter et al., 1971, 1975) is not explicitly included. Nevertheless in order to allow for a substantially larger evapotranspiration when the canopies are wet (without obviously explicitly accounting for the disappearance of the stomatal resistance (Shuttleworth, 1979)), the following succession of operations is followed.

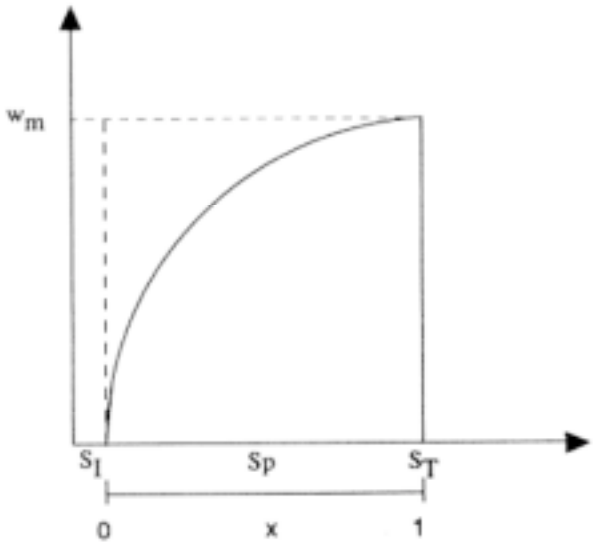

Fig. 2. Cumulative distribution for the elementary area soil moisture at saturation

If the precipitation P is larger than the potential evapotranspiration ET_p, the actual evapotranspiration, for the reasons expressed above, is assumed to coincide with the potential, i.e.:

$$ET_a = ET_p \tag{6}$$

and so an "effective" meteorological input M_e , defined as the difference between precipitation and potential evapo-transpiration, becomes:

$$M_e = P - ET_p = P - ET_a > 0 \tag{7}$$

With reference to Figure 3, the surface runoff R generated by the entire catchment is obtained as the sum of two terms, the first one is the product of the meteorological effective input and the percentage of impervious area while the second one is the average runoff produced by the pervious area, which is obtained by integrating the soil moisture capacity curve, which gives:

$$R = \frac{S_I}{S_T} M_e + \frac{S_T - S_I}{S_T} \int_w^{M_e + w} x(\xi) d\xi \tag{8}$$

if $M_e + w < w_m$, or

$$R = \frac{S_I}{S_T} M_e + \frac{S_T - S_I}{S_T} \left\{ M_e - \int_w^{w_m} [1 - x(\xi)] d\xi \right\} \tag{9}$$

if $M_e + w \geq w_m$.

Equations (8) and (9), can also be expressed in terms of the catchment average soil moisture content W and that at saturation W_m and after integration they become

$$R = M_e + \frac{S_T - S_I}{S_T} \left\{ (W_m - W) - W_m \left[\left(1 - \frac{W}{W_m} \right)^{\frac{1}{b+1}} - \frac{M_e}{(b+1) W_m} \right]^{b+1} \right\} \tag{10}$$

if $0 < M_e < (b+1) W_m \left(1 - \frac{W}{W_m} \right)^{\frac{1}{b+1}}$, or

$$R = M_e - \frac{S_T - S_I}{S_T} (W_m - W) \tag{11}$$

if $M_e \geq (b+1) W_m \left(1 - \frac{W}{W_m} \right)^{\frac{1}{b+1}}$.

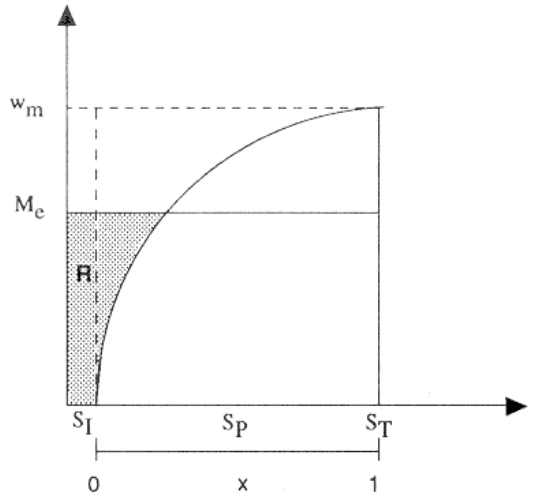

Fig. 3. Runoff *R* generated by an effective meteorological input $M_e>0$.

If the precipitation P is smaller than the potential evapotranspiration ET_p the effective meteorological input M_e, becomes negative:

$$M_e = P - ET_p < 0 \tag{12}$$

which implies that the runoff R is zero. The actual evapotranspiration is then computed as the precipitation P plus a quantity which depends upon M_e reduced by the average degree of saturation of the soil, which gives:

$$ET_a = P + (ET_p - P)\frac{(S_T - S_I)}{S_T}\frac{\left(1+\frac{W}{W_m}\frac{1}{b}\right)-\left(1-\frac{W}{W_m}\right)^{\frac{1}{b+1}}}{\left(1+\frac{1}{b}\right)-\left(1-\frac{W}{W_m}\right)^{\frac{1}{b+1}}} \tag{13}$$

These equations, which represent the average surface runoff produced in the sub-catchment, must be associated with an equation of state in order to update the mean water content in the soil. This equation takes the form:

$$W_{t+\Delta t} = W_t + P - ET_a - R - D - I \tag{14}$$

where all the quantities represent averages over the sub-basin and are expressed in mm:

$W_{t+\Delta t}$	is the soil moisture content at time $t+\Delta t$;
W_t	is the soil moisture content at time t .
P	is the area precipitation between t and $t+\Delta t$;
ET_a	is the evapotranspiration loss between t and $t+\Delta t$;
R	is the total runoff between t and $t+\Delta t$;
D	is the loss through drainage between t and $t+\Delta t$;
I	is the percolation loss between t and $t+\Delta t$;

The non-linear response of the unsaturated soil to precipitation, represented by the shape of the distribution curve given by equation (5), is strongly affected by the horizontal drainage and vertical percolation losses. The drainage loss D is an important quantity to be reproduced in a hydrological model, since on the one hand it affects the soil moisture storage and on the other hand it controls the hydrograph recession. Theoretical considerations on the unsaturated zone flow as well as application results have suggested in time various types of empirical relationships to express the drainage loss D as a non-linear function of the soil moisture. The most recently adopted expression in the ARNO model is the following, which although written as a lumped equation valid at catchment scale, looks similar to the one, valid at a point, which is due to Brooks and Corey (1964):

$$D = D_s \left(\frac{W}{W_m} \right)^{c1} \tag{15}$$

where

$\frac{W}{W_m}$ is the percentage saturation;

$c1$	is an exponent related to the soil types;
D_s	is the drainage at saturation;

The percolation loss I, which feeds the groundwater module, is represented with a similar expression, although generally with different parameters. which will control the base flow in the

model, varies less significantly over time if compared with the other terms; nevertheless a non-linear behaviour is also assumed as follows:

$$I = I_s \left(\frac{W}{W_m} \right)^{c2} \tag{16}$$

$c2$ = exponent related to the soil types;

I_s = infiltration at saturation;

The total runoff per unit area produced by the precipitation P is finally expressed as:

$$R_{tot} = R + D + B \tag{17}$$

where:

B is the base flow generated by the presence of a groundwater table fed by the percolation, and computed by the groundwater module.

2.2. The Evapotranspiration Module

In the ARNO model, a second forcing factor is provided by evapotranspiration, which can be either computed externally and directly introduced as an input to the model or estimated internally as a function of the air temperature. The internal evapotranspiration estimator uses in fact a simplified technique which has proven more than accurate for modelling the rainfall runoff process, where evapotranspiration plays a major role not really in terms of its instantaneous impact, but in terms of its cumulative temporal effect on the soil moisture volume depletion; this reduces the need for an extremely accurate expression, provided that its integral effect be well preserved. Although acknowledging the fact that the Penman-Monteith equation is the most rigorous theoretical description for this component, for a practical utilisation a simplified approach is generally necessary because in most countries the required historical data for its estimation are not extensively available, and, in addition, apart from a few meteorological stations, almost

nowhere are real time data available for flood forecasting applications. In the ARNO model, the effects of the vapour pressure and wind speed are explicitly ignored and evapotranspiration is calculated starting from of a simplified equation known as the radiation method (Doorembos et al., 1984):

$$ET_{0d} = C_v W_{ta} R_s = C_v W_{ta} \left(0.25 + 0.50 \frac{n}{N} \right) R_a \qquad (18)$$

where:

ET_{0d} is the reference evapotranspiration, i.e. evapo-transpiration in soil saturation conditions caused by a reference crop (mm/day) ;

C_v is an adjustment factor obtainable from tables as a function of the mean wind speed;

W_{ta} is a compensation factor that depends on the temperature and altitude;

R_s is the short wave radiation measured or expressed as a function of R_a in equivalent evaporation (mm/day);

R_a is the extraterrestrial radiation expressed in equivalent evaporation (mm/day);

n/N is the ratio of actual hours of sunshine to maximum hours of sunshine (values measured or estimated from mean monthly values).

Hence the calculation of R_s requires both knowledge of R_a, obtainable from tables as a function of latitude, and knowledge of actual n/N values, which may not be available. In the absence of the measured short wave radiation values R_s or of the actual number of sunshine hours otherwise needed to calculate R_s as a function of R_a (see equation (18)), an empirical equation was developed that relates the reference potential evapotranspiration ET_{0d}, computed on a monthly basis using one of the available simplified expressions such as for instance the one due to Thornthwaite and Mather (1955), to the compensation factor W_{ta}, the mean recorded temperature of the month T and the maximum

number of hours of sunshine *N*. The developed relationship is linear in temperature (and hence additive), and permits the dissaggregation of the monthly results on a daily or even on an hourly basis, while most other empirical equations are ill-suited for time intervals shorter than one month.

The relation used, which is structurally similar to the radiation method formula in which the air temperature is taken as an index of radiation, is:

$$ET_0 = \alpha + \beta N W_{ta} T_m \tag{19}$$

where:

ET_0 is the reference evapotranspiration for a specified time step Δt (in mm/Δt);

α, β are regression coefficients to be estimated for each sub-basin;

T_m is the area mean air temperature averaged over Δt;

N is the monthly mean of the maximum number of daily hours of sunshine (tabulated as a function of latitude).

W_{ta} for a given sub-basin can be either obtained from tables or approximated by a fitted parabola:

$$W_{ta} = A\overline{T}^2 + B\overline{T} + C \tag{20}$$

where:

A, B, C are coefficients to be estimated;

$\overline{T}$ is the long term mean monthly sub-basin temperature (^{o}C).

2.3. The Snowmelt Module

Again, for reasons of limited data availability, in the ARNO model the snowmelt module is driven by a radiation estimate based upon the air temperature measurements; in practice the inputs to the module are the precipitation, the temperature, and the same radiation approximation which is used in the evapotranspiration module.

Given the role that altitude may play in combination with the thermal gradient, the sub-catchment area is subdivided into a number of equi-elevation zones (snow-bands) according to the hypsometric curve, and for each zone simplified mass and energy budgets are continuously updated. For each snowband the following steps, similar to those adopted in SHE (Abbott et al., 1986), are followed:

- Estimation of radiation at the average elevation of the snowband;
- Decision whether the precipitation is solid or liquid;
- Estimation of the water mass and energy budgets based on the hypothesis of zero snowmelt;
- Comparison of the total available energy with that sustained as ice by the total available mass at 273 °K;
- Computation of the snowmelt produced by the excess energy; and updating the water mass and energy budgets.

2.3.1. Estimation of radiation at the average elevation of the snowband

The estimation of the radiation is performed by re-converting the latent heat (which has already been computed as the reference evapotranspiration ET_0) back into radiation, by means of a conversion factor C_{er} (Kcal Kg^{-1}) which can be found in any thermodynamics textbook as:

$$C_{er} = 606.5 - 0.695\left(T - T_0\right) \tag{21}$$

where T_0 is the temperature of fusion of snow (273 °K).

In addition, in order to account for albedo which plays an extremely important role in snowmelt, it is necessary to apply an efficiency factor which will be assumed approximately as η = .6 for clear sky and η = .8 for overcast conditions: this leads to the following estimate for the driving radiation term:

$$Rad = \eta\left[606.5 - 0.695\left(T - T_0\right)\right]ET_0 \tag{22}$$

Given the lack of information concerning the status of the sky when simulating with historical data, for practical purposes it

is generally assumed in the ARNO model that the sky is clear if there is no precipitation and overcast if precipitation is being measured.

2.3.2. Decision whether the precipitation is solid or liquid

Information concerning the status of precipitation (solid or liquid) is rarely available as a continuous record; therefore it is necesary to define a mechanism, mainly based upon the air temperature measurements and the historical precipitation. If one plots the frequency of the usually scattered observations with which precipitation was observed to be liquid or snow as a function of the air temperature, a Gaussian distribution is generally obtained, with a mean value T_s which very seldom will coincide with T_0. For this reason, the following rules are adopted:

- Precipitation is taken as liquid if the air temperature $T > T_S$;
- Precipitation is taken as snow otherwise.

The value of T_S (which generally ranges between 271 and 275 °K) must be derived, as previously mentioned, by plotting the frequency of the status of historically recorded precipitation as a function of the air temperature.

2.3.3. Estimation of the water and energy budgets on the hypothesis of zero snowmelt

The water equivalent mass is estimated with the following simple mass balance equation, where all quantities are expressed in mm of water:

$$Z^*_{t+\Delta t} = Z_t + P \qquad (23)$$

The water equivalent at the end of the time step is designated with a star because it is a tentative value which does not yet account for the eventual snowmelt.

Similarly to the mass, the energy is estimated in the following way, by computing the increase (or decrease) of total energy E:

- if the precipitation is zero:

$$E^*_{t+\Delta t} = E_t + Rad \tag{24}$$

-if the precipitation is non-zero and the precipitation is in the solid phase ($T \le T_{sn}$)

$$E^*_{t+\Delta t} = E_t + Rad + C_{sg} T_0 P \tag{25}$$

-if the precipitation is non-zero and the precipitation is in the liquid phase ($T > T_{sn}$)

$$E^*_{t+\Delta t} = E_t + Rad + \left[C_{si} T_0 + C_{lf} + C_{sa}(T - T_0)\right]P \tag{26}$$

Again the total energy at the end of a time step is designated with a star to denote a tentative value; in the previous equations C_{si} is the specific heat of ice (0.5 Kcal °K^{-1} Kg^{-1}), C_{lf} the latent heat of fusion of water (79.6 Kcal Kg^{-1}) and C_{sa} the specific heat of water (1 Kcal °K^{-1} Kg^{-1}).

2.3.4. Estimation of snowmelt and updating of mass and energy budgets

If the total available energy is smaller or equal to that required to maintain the total mass in the solid phase at the temperature T_0 i.e; $C_{si} Z^*_{t+\Delta t} T_0 \ge E^*_{t+\Delta t}$,it means that the available energy is not sufficient to melt part of the accumulated water, and therefore:

$$\begin{cases} R_{sm} = 0 \\ Z_{t+\Delta t} = Z^*_{t+\Delta t} \\ E_{t+\Delta t} = E^*_{t+\Delta t} \end{cases} \tag{27}$$

where R_{sm} is the snowmelt expressed in mm. If the total available energy is larger than that required to maintain the total mass in the solid phase at the temperature T_0 , it means that part of the accumulated water will melt, and therefore the following energy balance equation holds:

$$C_{si}\left(Z^*_{t+\Delta t} - R_{sm}\right)T_0 = E^*_{t+\Delta t} - \left(C_{si} T_0 + C_{lf}\right)R_{sm} \tag{28}$$

from which the snowmelt and the mass and energy state variables can be computed as:

$$\begin{cases} R_{sm} = \dfrac{E^*_{t+\Delta t} - C_{si} T_0 Z^*_{t+\Delta t}}{C_{lf}} \\ Z_{t+\Delta t} = Z^*_{t+\Delta t} - R_{sm} \\ E_{t+\Delta t} = E^*_{t+\Delta t} - \left(C_{si} T_0 + C_{lf}\right) R_{sm} \end{cases} \tag{29}$$

2.4. The Groundwater Module

The groundwater module represents the overall response of its storage by means of a cascade of linear reservoirs, characterised by two parameters: the number of reservoirs *n* and their time constant *K* , a model which is well known in hydrology as the Nash model (Nash, 1958). For practical reasons, instead of using the Gamma distribution function to express the impulse response, a numerical procedure has been adopted. The expression to be used can easily be derived from the assumption of a cascade of linear reservoirs where the volume of the i^{th} reservoir is proportional to its outflow, i.e. $S_t = K B_t^i$; thus, the continuity equation written for the generic ith reservoir becomes:

$$K \frac{\partial B_t^i}{\partial t} = B_t^{i-1} - B_t^i \tag{30}$$

which, after discretization in time with a finite difference scheme centred at time $t+\Delta t/2$, becomes:

$$\frac{K}{\Delta t}\left(B_{t+\Delta t}^i - B_t^i\right) = \frac{B_{t+\Delta t}^{i-1} + B_t^{i-1}}{2} - \frac{B_{t+\Delta t}^i + B_t^i}{2} \tag{31}$$

and the required expression is then obtained by making $B_{t+\Delta t}^i$ explicit:

$$B_{t+\Delta t}^i = \frac{2K - \Delta t}{2K + \Delta t} B_t^i + \frac{\Delta t}{2K + \Delta t}\left(B_{t+\Delta t}^{i-1} + B_t^{i-1}\right) \tag{32}$$

where:

B^i is the outflow from the ith reservoir

$B^0 = I$ is the percolation given by the soil moisture balance

equation

$B^n = B$ is the resulting base flow

Equation (32) is then recursively solved n times at each time step.

2.5. The Parabolic Routing Module

The routing in the ARNO model is performed by assuming for the catchment the "open book" shape, as shown in Figure 4 and dividing the routing problem into a sequence of three separate linear routings. The first one relates to the routing to the main channel of the total runoff, given by equation (17) and assumed to be uniformly produced over the hillslopes on a unit width strip; the second one relates to the routing in the main channel of the distributed inflow (per unit width strip) produced by the hillslopes; the third one, which is used to link together several sub-catchments, relates to the routing of upstream inflows to the exiting section of the downstream sub-catchment. The three steps are illustrated in Figure 4 and described in the sequel.

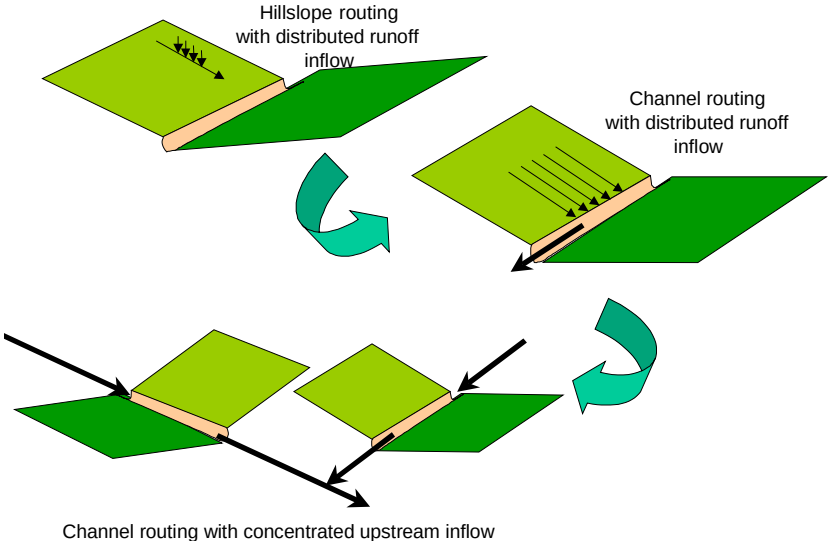

Fig. 4. Schematic representation of the three steps in routing

The hillslope routing and channel routing of distributed

inflows are both performed using a distributed input linear parabolic model, while channel routing of upstream inflows to a downstream sub-basin is performed by means of a concentrated input parabolic model. The parameters of the two linear parabolic transfer functions can be estimated as a function of the slope, the length and the roughness of the drainage system.

2.5.1. Routing of upstream inflows

The propagation of inflows from upstream is carried out by means of a linear model consisting of a parabolic unit hydrograph deriving from the analytical integration of the unsteady flow equations when the inertia effects are ignored and the coefficients are linearised around mean outflow values. In this case the following differential equation is obtained:

$$\frac{\partial Q}{\partial t} = D\frac{\partial^2 Q}{\partial x^2} - C\frac{\partial Q}{\partial x} \tag{33}$$

where D and C are the diffusivity and the convectivity coefficient respectively. The discrete time solution of equation (33) for mean values of the coefficients C and D is (Todini and Bossi, 1986):

$$\overline{U}_{\Delta x}(t, t+\Delta t) = \frac{1}{\Delta t^2}\left[IF(t+\Delta t) - 2IF(t) + IF(t-\Delta t)\right] \tag{34}$$

where

$$IF(t) = \int_0^t F(\vartheta)d\vartheta = \int_0^t\int_0^{\vartheta} u_{\Delta x}(\tau)d\tau d\vartheta \tag{35}$$

with $u_{\Delta x}$, the impulse response relevant to equation (35), which can be written as:

$$u_{\Delta x}(\tau) = \frac{\Delta x}{\sqrt{4\pi D\tau^3}} e^{-\frac{(\Delta x - C\tau)^2}{4D\tau}} \tag{36}$$

Integrating equation (35), after substitution from equation (36) one obtains:

$$IF(t)=\frac{1}{C}\left[(Ct-\Delta x)N\left(-\frac{\Delta x-Ct}{\sqrt{2Dt}}\right)+(Ct+\Delta x)e^{\frac{\Delta xC}{D}}N\left(-\frac{\Delta x+Ct}{\sqrt{2Dt}}\right)\right] \quad (37)$$

where *N(*)* is the value of the Standard Normal probability distribution in (*****), and Δx is the length of the channel reach.

2.5.2. Diffuse lateral inflow routing

The runoff generated in each sub-basin moves first along the slopes and then reaches the drainage network as diffuse inflow that, for simplicity, may be considered uniformly distributed. In this case the following differential equation applies:

$$D\frac{\partial^2 Q}{\partial x^2}-C\frac{\partial Q}{\partial x}-\frac{\partial Q}{\partial t}=-Cq \quad (38)$$

where q is the lateral inflow per unit length. The discrete time solution of equation (38) for mean values of the coefficients C and D is (Franchini and Todini, 1989):

$$\overline{UL}_{\Delta x}(t,t+\Delta t)=\frac{1}{\Delta t^2}\left[IG(t+\Delta t)-2IG(t)+IG(t-\Delta t)\right] \quad (39)$$

where:

$$IG(t)=\frac{C}{2}\left[t^2-IIF(t)\right] \quad (40)$$

with

$$IIF(t)=\int_0^t IF(\xi)d\xi=\int_0^t\int_0^\xi F(\vartheta)d\vartheta d\xi=\int_0^t\int_0^\xi\int_0^\vartheta u_{\Delta x}(\tau)d\tau d\vartheta d\xi \quad (41)$$

Integration of equation (41), after substitution of $u_{\Delta x}$ from equation (36), yields:

$$IG(t)=\frac{C}{2}\left\{t^2-\left(t^2+\frac{\Delta x^2}{C^2}\right)\left[N\left(-\frac{\Delta x-Ct}{\sqrt{2Dt}}\right)+N\left(-\frac{\Delta x+Ct}{\sqrt{2Dt}}\right)e^{\frac{\Delta xC}{D}}\right]\right\}+$$
$$+\frac{C}{2}\left\{\frac{2\Delta x}{C}\left(t-\frac{\Delta x}{C^2}\right)\left[N\left(-\frac{\Delta x-Ct}{\sqrt{2Dt}}\right)-N\left(-\frac{\Delta x+Ct}{\sqrt{2Dt}}\right)e^{\frac{\Delta xC}{D}}\right]\right\}+ \quad (42)$$
$$+\frac{C}{2}\left\{\frac{2\Delta x}{C^2}\sqrt{\frac{Dt}{\pi}}e^{-\frac{(\Delta x-Ct)^2}{4Dt}}\right\}$$

The results provided by equation (38) when substitued for *IG(t)* given by equation (42), differ from the ones obtained by Naden (1992), in that they represent the response of a discrete time system to a time discretised input (see Todini and Bossi, 1986).

3. THE ARNO MODEL PARAMETERS

All the ESMA type models require calibration of several of parameters. Some of these parameters relate to the main processes, such as the soil moisture dynamical balance, and play an important role in the model performances in that they may modify the output by an order of magnitude. Other parameters, such as for instance the routing parameters, will only affect the timing of the response or may produce errors of the order of 10-20%. This is why the comparison among the different ESMA type models, is generally based upon the soil component parameters.

In the ARNO model, the following parameters are soil component parameters that require accurate calibration by means of historical data and verification using split sample testing techniques:

W_m represents the average volume in mm of soil moisture storage. This parameter can be derived as a function of the soil types and its value ranges in general from 50 to 350 mm;

b represents a shape factor for the soil moisture vs saturated areas curve; its value, which ranges between .01 and .5, is

somehow related to the soil types and their spatial variability, but must be estimated from the data.

D_s is the maximum drainage (in mm per time unit) that should be expected when the soil is completely saturated; it is a function of many factors including the geo-morphological structure of the catchment, the soil types, the space and time scales of the problem, and must be estimated from the data.

c1 exponent (which depends on soil types with values ranging generally between 1.5 and 3) used to represent drainage when saturation is not reached which value is estimated from historical data.

I_s is the maximum percolation (in mm per time unit) that should be expected when the soil is completely saturated; similarly to D_s it depends upon several items and must be estimated from the data.

c2 exponent (which depends on soil types with values ranging generally between 1 and 2) used to represent percolation when saturation is not reached which value is estimated from historical data.

Other parameters appearing in the equations, such as S_T, S_P and S_I, do not require estimation from historical data, but can be directly evaluated on the basis of geo-morphological, soil and land use maps.

The ARNO model is therefore essentially based upon 6 parameters, a small number when compared to more classical ESMA type models (generally more than 20 parameters), but still the double of the parameters required in the TOPMODEL (Beven and Kirkby, 1979). Moreover, although related to the problem physics, not all the ARNO model parameters can be directly estimated or derived from maps, which is the major model limitation when wishing to use the model on ungauged catchments.

As mentioned earlier, the estimation of the parameters relevant to the routing model components (hillslopes and

channels) are not critical. A convectivity *C* and diffusivity *D* coefficient must be provided for each response function which value may be related to the dimensions, slopes and lengths of the individual sub-basins. In general very small values for *D* are assumed for the hillslopes, given the marked kinematic nature of the phenomenon; generally, *D* increases with the size of the river and with the inverse of the bottom slope. Table 1 gives an indication of the orders of magnitude of *C* and *D*.

	C (m/s)	*D(m^2/s)*
Hillslopes	1-2	1-100
Brooks	1-3	100-1000
Rivers	1 - 3	1000-10000
Large rivers	1 - 3	10000-100000

Table 1 -Approximate initial guess for parameters C and D.

4. APPLICATION OF THE ARNO MODEL

Since its derivation, the ARNO model, given its simplicity and robustness, was used in various parts of the world as the basic tool for the development of several real-time operational flood forecasting systems. Moreover, the soil moisture balance component was successfully used as an alternative to the Manabe (1969) soil bucket in the several GCMs, such as the ECHAM2 model (Dümenil and Todini, 1992, Roeckner et al., 1992), the UK Meteorological Office (UKMO) model (Rowntree and Lean, 1994), and the LMD model (Polcher et al., 1995) while modified versions of the ARNO model have also been developed such as for instance the VIC model by Wood et al. (1992) who extended the ARNO model concepts to multiple soil layers or the ADM model (Franchini and Galeati, 1997) a simplified version of the ARNO.

Fig. 5. The river Tiber catchment and the sub-basins

From the application point o view, several rivers have been successfully modelled by means of the ARNO model: the Fuchun river in China, the Danube river in Germany, and the rivers Arno, Tiber, Fortore, Ofanto, Adda, Ticino, Oglio, Agno-Guà, Tronto in Italy. In order to illustrate the ARNO model performances, only its application to the case of the real time flood forecasting system of the river Tiber will be described.

The Tiber, the third largest river in Italy, is 403 km long with a catchment area of over 17,000 km^2 originating from Mount Fumaiolo at an altitude of 1260 m a.s.l. and debauching into the Thyrrenean sea near Rome, the capital of Italy.

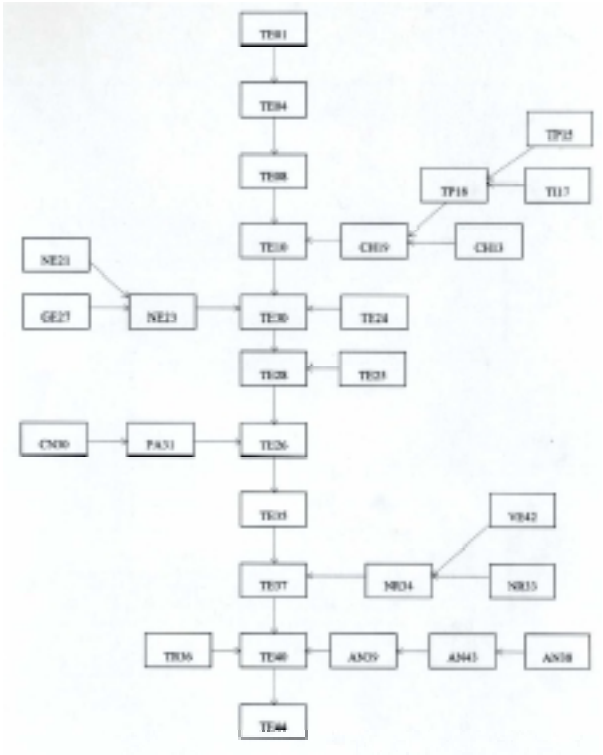

Fig. 6. The schematic representation of river Tiber catchment and its sub-basins in the ARNO model

Figure 5 shows a map of the Tiber basin which was divided in 30 sub-basins in order to set up the ARNO model. This subdivision is required for three main reasons. The first one relates to the need of preserving homogeneity in the geo-morphological and meteo-climatical characteristics in the different sub-units over which the processes are lumped (which generally requires sub-units of a few hundred square kilometres in size); the second one relates to the availability of rating curves for the calibration of the different model components; the third one is imposed by the sections of interest, namely the river cross sections for which the computations or the forecasts are needed. Figure 6 shows the interconnections of the different sub-units used in the ARNO model for the development of the single rainfall-runoff models and for their routing to the river mouth.

Continuous records of hydro-meteorological data from June 1993 to May 1994 were available at 47 rain gauge stations, 18 thermometric stations and 22 level gauge stations and used for the calibration of the ARNO model.

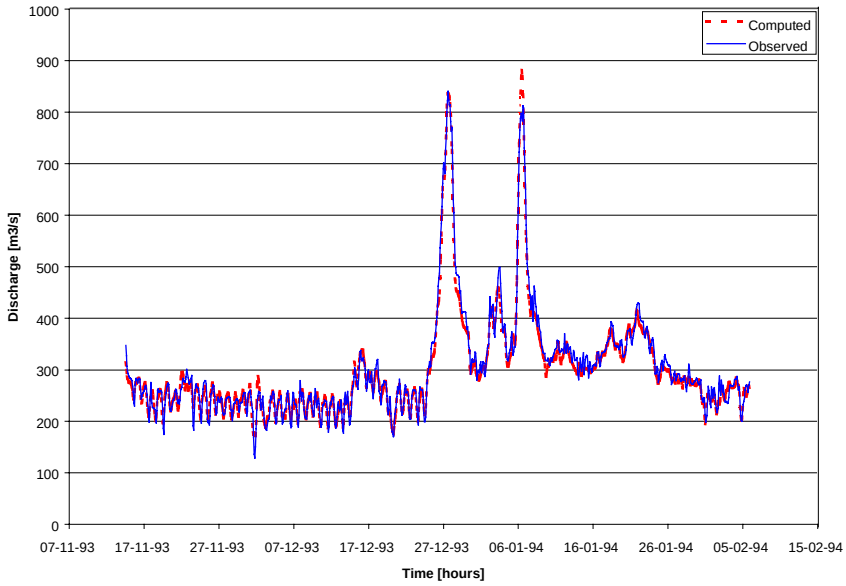

Fig. 7. Calibration results for a flood period at Rome Ripetta station

Figure 7 shows the calibration results obtained in the flood period at the ending section of Rome Ripetta where 12 hours advance forecasts are needed in order to close a number of sluices thus avoiding the waters to flow into the city streets. The figure also shows that the model also captured the marked effect of the upstream reservoir of Corbara, which is located in the middle part of the Tiber, and which affects particularly the low flows. A model for the reservoir had to be implemented and used as an additional module in the ARNO model. The quality of the calibration was considered as successful with over 95% of explained variance. The calibrated parameters were then used for the development of a real time flood forecasting system based on EFFORTS (European Flood Forecasting Operational Real Time System) (ET&P, 1992) which includes the ARNO model

together with other models such as the hydraulic flood routing model PAB (Todini and Bossi, 1986) and the Kalman filter based error model MISP (Todini, 1978).

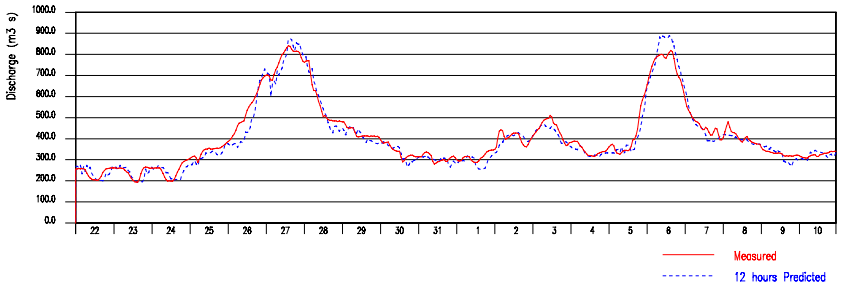

Fig. 8. Simulated real time 12 hours in advance forecasts compared to the measured discharges on the Tiber at Rome Ripetta.

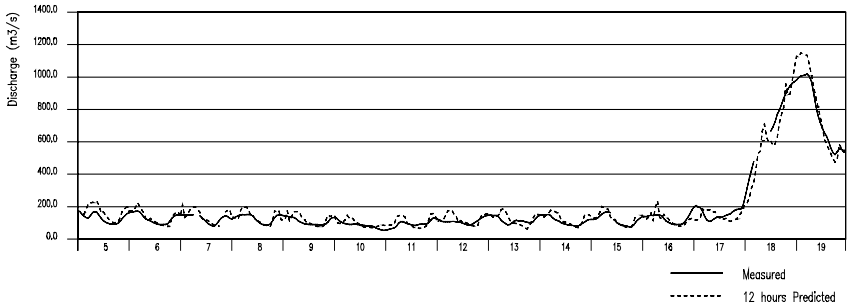

Fig. 9. Operational real time 12 hours in advance forecasts compared to the measured discharges on the Tiber at Rome Ripetta.

The quality of the real time forecasting results is illustrated in Figure 8 comparing the measured values with the succession of 12 hours in advance simulated real time flood forecasts at Rome Ripetta station during the flood period in the calibration record.

The system was then operationally installed in October 1994 and figure 9 compares the measured values with the succession of 12 hours in advance, this time operational, real time flood forecasts at Rome Ripetta station during November 1994, showing practically the same pattern of reliable 12 hours in advance flood forecasts.

5. CONCLUSIONS

The ARNO model described in this paper has proven to be a reliable and flexible tool for rainfall-runoff modelling at catchment or at sub-catchment scale as shown by the numerous successful applications on large and complex rivers as well as on small and flash flood prone brooks. The model parameterisation is a compromise between the complexity and space and time variability of phenomena to be reproduced and the simplicity offered by its lumped formulation.

The limitations of the approach lie mainly in the lack of direct interpretation of some of its parameters that do not allow for the extension of model calibration to ungauged catchments. On the other hand, when long records of rainfall and runoff are available, the model can be successfully calibrated and used both for simulation and for real time flood forecasting.

In order to overcome the above mentioned limitations while preserving the ARNO model contributing areas dynamics, further studies have indicated the possibility of deriving a new generation of distributed models such as for instance the TOPKAPI (Todini and Ciarapica, 2001), which parameters are physically based and calibration is possible on the basis of digital elevation, soil and land use maps; but showing the interesting characteristics of collapsing into a model similar to the ARNO model, when lumped at catchment or at sub-catchment scales.

6. REFERENCES

Abbott, M.B., Bathurst, J.C., Cunge, J.A., O'Connell, P.E. and Rasmussen, J., 1986a, An introduction to the European Hydrological System - Système Hydrologique Européen, "SHE", 1: History and philosophy of a physically-based, distributed modelling system. J. Hydrol., 87: 45-59; 2: Structure of physically-based, distributed modelling system. J. Hydrol., 87: 61-77.

Beven K.J. and Kirkby M.J.. 1979 A physically based, variable contributing area model of basin hydrology. Hydrol. Scien. 24: 1-3.

Brooks R.H., Corey A.T., 1964. Hydraulic properties of porous media,. Hydrol. Pap. 3. Colo. State Univ., Fort Collins.

Crawford, N.H. and Linsley, R.K., 1966. Digital simulation in hydrology, Stanford Watershed Model IV. Stanford Univ. Dep. Civil. Eng. Rep. 39.

Dooge, J.C.I., 1973. The linear theory of hydrologic systems. US. Dep. Agric. Tech. Bull., 1468.

Doorembos J., Pruitt W.O., Aboukhaled A., Damagnez J., Dastane N.G., van den Berg C., Rijtema P.E., Ashford O.M., Frere M., 1984. Guidelines for predicting crop water requirements. FAO Irrig. Drainage Pap., 24.

Dümenil L. and Todini E., 1992. A rainfall-runoff scheme for use in the Hamburg climate model. In J.Ph.O'Kane (Editor), Advances in Theoretical Hydrology - A tribute to James Dooge. Elsevier, Amsterdam.

ET&P, 1992. The Fuchun River project - A computer based real time system - EC-China Cooperation. Final Report Research Contract n. CI13-0004-I (A), Bologna.

Franchini, M. and Pacciani, M., 1991. Comparative analysis of several conceptual rainfall runoff models. J. Hydrol., 122: 161-219.

Franchini, M. and Todini, E., 1989. PABL: a parabolic and backwater scheme with lateral inflow and outflow. Fifth IAHR International Symposium on Stochastic Hydraulics, Report No. 10, Institute for Hydraulic Construction, University of Bologna.

Franchini, M. and Galeati G. 1997. Comparing several generic algorithm schemes for the calibration of conceptual rainfall-runoff models. Hydrol. Sci. J., 42(3), 357-379.

Manabe, S., 1969. Climate and ocean circulation: I. The atmospheric circulation and the hydrology of the Earth's surface. Mon. Weather Rev., 97: 739-774.

Moore, R.J., 1985. The probability-distributed principle and runoff production at point and basin scales. Hydrol. Science Journal, 30(2): 273-297.

Moore, R.J. and Clarke, R.T., 1981. A distribution function approach to rainfall-runoff modelling. Water Resour. Res., 17(5): 1367-1382.

Naden, P.S., 1992. Spatial variability in flood estimation for large catchments: the exploitation of channel network structure. Hydrol. Sciences Journal, 37(1-2):53-71.

Nash, J.E., 1958. The form of the instantaneous unit hydrograph. IUGG General Assembly of Toronto, Vol. III - IAHS Publ., 45: 114-121.

Polcher, J., Laval, K., Dümenil, L., Lean, J. And Rowntree, P.R., 1995. Comparing three land surface schemes used in GCMs. J. Hydrol., submitted.

Roeckner, E., Arpe, K., Bengtsson, L., Brinkop, S., Dümenil, L., Esch, M., Kirk, E., Lunkeit, F., Ponater, M., Rochel, B., Sausen, R., Schlese, U., Schubert, S., and Windelband, M., 1992. Simulation of the present-day climate with the ECHAM model: Impact of model physics and resolution, MPI Tech. Rep. No. 93, Max-Planck-Institut für Meteorologie, Hamburg, FRG.

Rowntree, P.R., Lean, J., 1994. Validation of hydrological schemes for climate models against catchment data. J.

Hydrol. 155: 301-323.

Rutter, A.J., Kershaw, K.A., Robins, P.C. and Marton, A.J., 1971. A predictive model of rainfall interception in forests. I: Derivation of the model from observations in a plantation of Corsican Pine , Agric. Meteorol., 9: 367.

Rutter , A.J., Marton, A.J. and Robins, P.C. , 1975. A predictive model of rainfall interception in forests. II: Generalisation of the model and comparison with observations in some coniferous and hardwood stands. J. Appl. Ecol., 12: 367.

Shuttleworth , W.J., 1979. Evaporation. Rep. 56, Institute of Hydrology, Wallingford.

Thornthwaite, C.W. and Mather, J.R., 1955. The water balance. Publ. in Climatology, 8(1) Lab. of Climatology, Centerton, N.J.

Todini E. and Wallis J.R. 1977. Using CLS for daily or longer period rainfall - runoff modelling - in Ciriani T.A., Maione U., Wallis J.R. (eds.) "Mathematical models for surface water hydrology" - John Wiley & Sons, London, pp.149-168.

Todini E. 1978. Mutually Interactive State/Parameter Estimation (MISP) - in Chao-Lin Chiu (ed.) "Application of Kalman Filter to Hydrology, Hydraulics and Water Respurces", University of Pittsburgh, Penn, pp. 135-151.

Todini, E., Bossi, A., 1986. PAB (Parabolic and Backwater), an unconditionally stable flood routing scheme particularly suited for real time forecasting and control. J. Hydraul. Res., 24(5): 405-424.

Todini E., 1988. Il modello afflussi deflussi del fiume Arno. Relazione Generale dello studio per conto della Regione Toscana, Technical Report, Bologna (in Italian).

Todini, E., 1996. The ARNO rainfall-runoff model. J Hydrol., 175: 339-382.

Todini, E. and Ciarapica L., 2001. The TOPKAPI model in Mathematical Models of Large Watershed Hydrology,

Chapter 12, edited by V. P. Singh, D. K. Frevert and S. P. Meyer, Water Resources Publications, Littleton, Colorado, in press.

World Meteorological Organization (WMO), 1975. Intercomparison of conceptual models used in operational hydrological forecasting. Operational Hydrology Rep. 7; WMO 429. WMO, Geneva.

Wood, E. P., D. P. Lettenmaier and V. G. Zartarian, 1992, A Land-surface hydrology parameterization with subgrid variability for general circulation models. J. Geophys. Res., 97 (D3), 2717-2728.

Zhao, R.J., 1977. Flood forecasting method for humid regions of China. East China College of Hydraulic Engineering, Nanjing, China.

Zhao, R.J., 1984. Watershed Hydrological Modelling. Water Resources and Electric Power Press, Beijing.